Defence Science Journal, Vol. 74, No. 6, November 2024, pp. 950-957, DOI : 10.14429/dsj.74.19865

Performance Prediction of Composite Marine Propeller Under The Influence of Hull Wake

Ashok Kumar* and R. Vijayakumar

Department of Ocean Engineering, IIT Madras, Chennai - 600 036, India
E-mail: s.ashokji@gmail.com

ABSTRACT

In the recent past, several improvements in the design, development, material selection and manufacturing of marine propellers were achieved by improving higher performance. Adaptive propellers are being chosen as an alternative to the conventional marine propeller. Several alternative materials were proposed as a replacement for conventional metals or alloys. However, only limited materials exhibited their superior performance and were found to be beneficial. This paper aims to investigate the performance of adaptive propellers under the influence of wake conditions. Three materials were considered as candidate propeller materials, namely, Aluminium (Al), Carbon Fibre Reinforced Plastic (CFRP), Glass Fibre Reinforced Plastic (GFRP). Reynolds Averaged Navier Stokes (RANS) equation-based Computational Fluid Dynamic (CFD) solver was adopted for estimating the hydrodynamic loads and transferred to a structural solver based on Finite Element Method (FEM) to compute the deformation and stresses. A Co-Simulation based Fluid Structure Interaction (FSI) coupling algorithm was adopted to compute the two-way FSI coupling between the solvers. Hydrodynamic coefficients, tip deflection and stresses were computed and reported for the wake condition.

Keywords: Hull wake; Composite propeller; Co-Simulation; B-series propeller

1. INTRODUCTION

The development of composite materials has enabled engineers to employ them in a wide range of applications, including the marine industry. The marine propeller is one of the essential parts of any ship/floater, which aids in providing forward thrust to move from one place to another. In several instances, composite materials replaced conventional propeller materials with their superior mechanical and chemical properties. Compared to traditional materials like aluminium, nickel, aluminium bronze, and manganese bronze, composite propellers perform better in hydrodynamics and hydroacoustic due to their high specific strengths, higher corrosion resistance and delayed cavitation inception speed. However, they are less preferred because of their low stiffness, anisotropic nature, lack of tested design techniques, and laborious production process. Until now, researchers have not fully explored the composite propeller's wake characteristics under the operating regime. Hence, it is essential to study the hull wake influence of composite propellers via fluid-structure interaction (FSI) analysis to comprehend the feasibility of using self-adaptive materials in the marine industry.

2. LITERATURE REVIEW

Very limited studies are available on the performance analysis of composite marine propeller (CMP)s in behind-hull conditions. He[1], *et al.* studied the characteristics of flexible propellers for reducing vibration and dynamic stresses using the CFD-FEM method under non-uniform wake conditions. Han[2], *et al.* the behind-hull performance of a composite KP458 propeller using the sliding mesh method and moving reference frame method for predicting the unsteady deformation under wake. Zondervan[3], *et al.* measured the deformation of a five-bladed flexible propeller using the Digital Image Corellation DIC technique behind the ship. The study aimed to establish the feasibility of using the DIC system to measure deformation during operating conditions. The study concluded that DIC had captured most of the blade surfaces with satisfactory levels of accuracy and suggested that optical fibre is more robust with greater accuracy in measurements. Grasso[4], *et al.* carried out one investigation on estimating the full-scale deflection of CMP under several operating conditions. Using DIC, tip deflection, noise and tip cavitation patterns were observed and reported. Numerically simulating the self-propulsion shall be tremendously costlier in terms of resource utilisation and simulation time. Several times, they are approximated using the virtual disk method for quicker and more reliable results. However, for CMPs, the blade profile must be used to estimate the exact performance prediction. Ashok[5–7], *et al.* studied vibration and self-propulsion characteristics of composite marine propellers using numerical simulations for a B series propeller at operating conditions in calm water. The deformation and stresses were reported to be lesser than in open water cases. Liang[8] performed hydrodynamic and hydroelastic analysis on the composite propeller with different stacking sequencing to

Received : 31 January 2023, Revised : 13 June 2024
Accepted : 14 June 2024, Online published : 25 November 2024

understand the performance. A literature review was conducted to collate the mechanism and various other phenomena which played a important part in analysing the performance of the marine propeller for three decades[9]. An extensive review was presented on the energy saving devices, vortex, cavitation, circulation, acoustic phenomena, including FSI of propellers. Wang[10], *et. al.* investigated the inception mechanism of propeller wake due to vortex interaction using detached eddy simulation method at two different advance ratios. The results indicated that the wake instabilities are due to the mutual induction of vortices from tip, trailing edge and high-speed shear layers. Also, the study revealed how tip vortices interact with other core vortices in uniform flow condition. Felli[11], *et al.* investigated velocity and pressure fields at the aft of propeller in non-cavitating regime using experimental method. Particle image velocimetry method used to investigate the velocities from the trailing edge up to two times diameter distances in downstream of the propeller. The study results proved that the tip vortices passage is very important aspect in generating the pressure field in the propeller. The deformation of hub vortex are due to the incoming vortices breakdown process which in turn causes pressure at shaft rate frequency.

Nouri[12], *et al.* investigated how the camber ratio affected the hydro-elastic performance of ducted propellers when a wake was present. Eight distinct propeller models with seven blades were subjected to the CFD-FEM-based coupling approach in order to evaluate hydrodynamic pressure, frequencies, deformation, and efficacy. At the operating regime, the camber ratio also enhances thrust; maximum efficiency was attained at camber ratio (f/c) = 1.5 %. An[13-14], *et al.* used modal analysis and two-way FSI simulations to study the hydro-elastic performance of a composite ducted propeller. Efficiency was influenced by the twist angle, which increases at lower J and decreases at higher J. Performance of propeller is greatly influenced by the tip clearance between the propeller tip and duct; larger gaps result in increased efficacy. A variation on the aforementioned work was done by Han[15], *et al.* using a different lamination strategy. Hussain[16], *et al.* found that pitch and skew had an impact on the propeller's twisting moment. In order to determine the performance changes, CFD analysis was first performed for rigid propellers and the geometric pitch was included. Efficiency at lower J was enhanced by the lower pitch. Additionally, the study showed that the design condition's positive pitching moment has a more capable self-adaptation. Using commercial CFD-FEM software, Fuentes[17], *et al.* conducted a monolithic FSI study for the P1790 propeller in open water settings. Characteristics related to hydrodynamics and hydroelasticity were assessed and contrasted with experimental findings. In this investigation, deformation patterns and stresses were noted and documented. Passive bending propellers' overall hydrodynamic performance has increased. Although several literature has documented the performance of the marine propeller especially composites, there were almost no literature available in open domain which records the wake influenced deformations. Such details are very critical to widen the horizon of propeller operation and optimisation at the very early stages of design. Thus, this study is found to be important and necessary.

The current work aims to understand the influence of hull wake on the composite marine propeller. RANSE-based CFD solver was adopted to compute the hydrodynamic performance and the FEM solver for the structural response. Three geometrically identical propellers made of Aluminium, CFRP and GFRP were designed based on the standard series diagram to operate at an advance ratio (J) of 0.5 for two different stacking sequences. The geometry was unaltered during manufacturing at static conditions. Initially, the hull parameters were identified using CFD and compared with experiments. The propeller performance was analysed in behind hull wake mode for the design speed. The blade tip deflection and stresses obtained for all the materials were compared with open water results. The influence of tip deflection on performance has also been studied.

2. GEOMETRICAL MODELS

The Wageningen B series four-bladed propeller and hull form for an ocean-going vessel was chosen as a candidate propeller and hull for the current investigation. The primary geometrical parameters are shown in Table 1. The numerical CAD model was developed using commercial 3D CAD software, as shown in Fig. 1. A numerical computational domain was designed with the propeller for the wet mode analysis and is shown in Fig. 2.

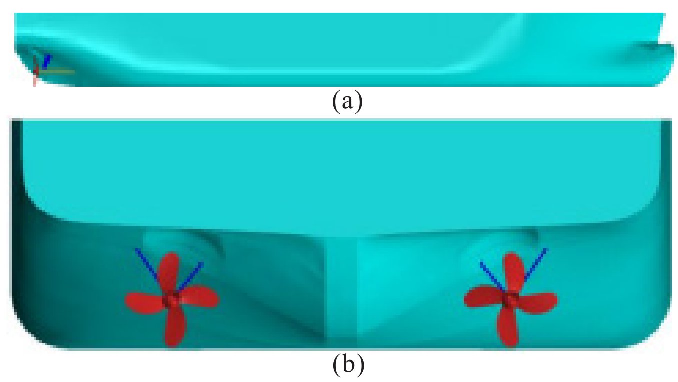

Figure 1. (a) 3D model of the hull; and (b) Propeller.

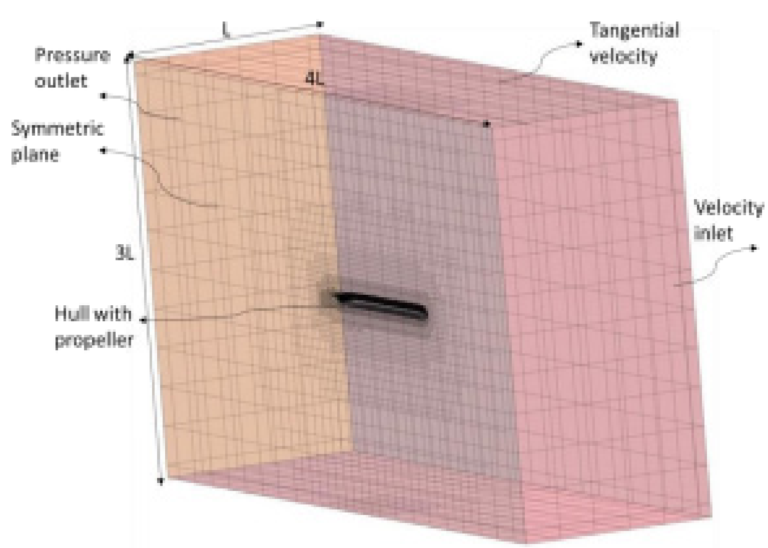

Figure 2. Computational domain.

Table 1. Geometrical properties of propeller

Diameter (D)	250 mm	Skew	0°
Pitch ratio (P/D)	0.826	Rake	0°
Expanded area ratio (A_E/A_O)	0.45	Hub ratio (d/D)	0.2

Due to the axisymmetric nature, only one-half of the underwater hull form and the propeller were used for the FSI numerical analysis. The dimensions are fixed in reference to the International Towing Tank Conference (ITTC) guidelines [ITTC (2014)]. The boundary conditions adopted for the study are presented in Fig. 2. The lab frame of reference was fixed at the keel, centreline, and transom intersection. The propeller reference line was fixed to the generator line of the propeller. Volumetric refinements were created near the hull and propeller zones for mesh refinements. Because the boundaries were kept far from the hull region, the wall effects on the CFD results were completely avoided.

Two regions were created for numerical simulation: stationary and rotating. The stationary region is the background region where the stationary hull generates the wake, and in the rotating region, the propeller is placed. Interfaces were created between regions that are crucial in transferring values from one region to another.

3. MESH AND BOUNDARY CONDITION

The current investigation considered three different materials: Aluminium 6061, Carbon Fibre Reinforced Plastic (CFRP) and Glass Fibre-Reinforced Plastic (GFRP).

3.1 Material Properties

The mechanical properties used to simulate the materials onto the propeller are tabulated below in Table 2 and stacking sequences in Table 3. The study has incorporated the direction dependencies on composite material for more accurate evaluation of performance characteristics.

3.2 Meshing

Mesh generation is crucial for any computer-based analysis as the mesh quality determines the results' accuracy. Two different mesh types were used for simulating hydrodynamic and hydro structural analysis. Unstructured trimmer cells were used in the stationary region of the domain, and a thin mesher was used for the rotating. To compute structural behaviour, an unstructured tetrahedral model was added to the solid model. The mesh of individual components and volumetric refinements were regulated as a percentage of base size, while the total meshing base size was kept constant at 1 m. At rotary interfaces, the mesh size was kept constant in both the rotatory and stationary zones. The information about the boundary layer for the hull and the propeller was obtained via prism layer meshing. The meshed propeller for Aluminium 6061 is shown below in Fig. 3. In FEM mode, Around 0.42 million nodes and 0.4 million elements were present. The speed of the propeller is 500 rpm.

The wall Y+ value was maintained at less than 5 throughout the simulations. The Morphing motion in CFD redistributes mesh vertices in response to the movement of control points[19]. The mesh Morpher uses control points and their associated

Table 2. Material properties of different propeller material

Material	ρ (kg/m³)	E_1 (GPa)	E_2 (GPa)	υ_{12}	G_{12}(GPa)	G_{23}(GPa)	G_{13}(GPa)
CFRP	1625	153.97	9.7	0.34	5.79	2.9	2.9
GFRP	2020	59	20	0.28	9	4.5	4.5

Table 3. Stacking sequence

Sequence A	$[0]_S$
Sequence B	$[0/30/45/-30/-45]_S$

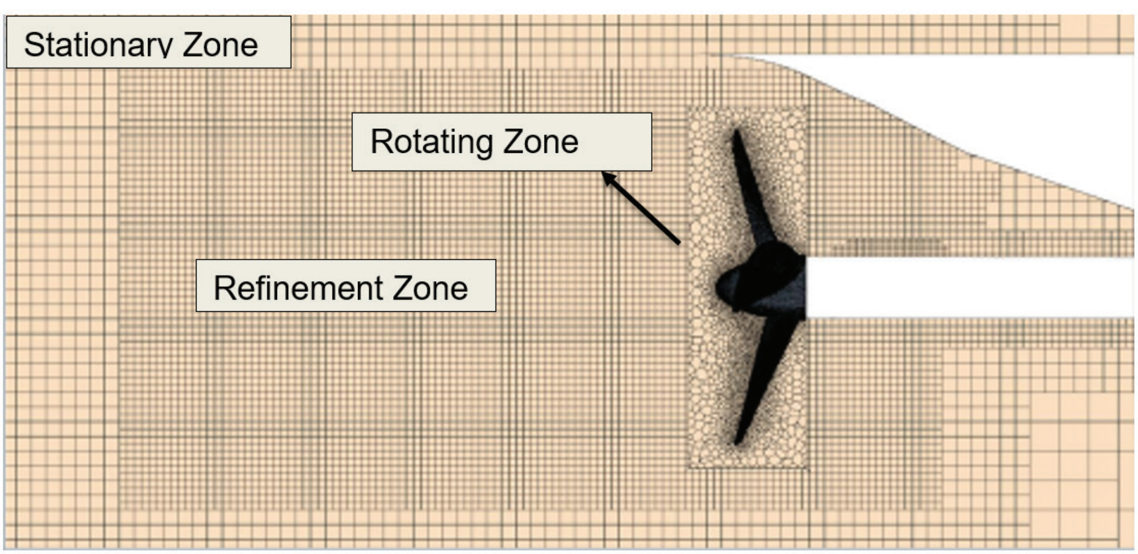

Figure 3. Meshed propeller blade.

Table 4. Grid convergence index (GCI)

Number of cells	N1	N2	N3
	6.11E+06	**2.16E+06**	**7.63E+05**
Absolute value	F1	F2	F3
	0.0795	0.0760	0.0750
Grid refinement ratio	r21		r32
	1.41		1.41
Absolute difference	v21		v32
	-0.0035		-0.0010
Apparent order	p	3.6335	
Extrapolated value	ϕext21		ϕext32
	0.0809		0.0764
Approximate relative error	ea21		ea32
	4.41 %		1.31 %
extrapolated relative error	eext21		eext32
	1.72 %		0.52%
Grid Convergence Index,GCI	GCI21		GCI32
	2.18 %		0.65 %

displacements to generate an interpolation field throughout the region, which can then be used to displace the actual vertices of the mesh.

The solution obtained purely depends on the mesh quality for any CFD analysis. High-quality meshing is required for minimising the discretisation error. The grid convergence index (GCI) has been chosen as a tool to measure the numerical uncertainty produced by discretisation error. The GCI is calculated using the method proposed by Roache[18]. Three grids with different refinements were considered for this study. The displacement was chosen as the performance parameter, and the grid refinement factor is maintained at greater than 1.414. The results of the GCI calculation are shown in Table 4, and the value across consecutive grids is near 0.7 %. Thus, it can be concluded that the solution is in the monotonic convergence range, and further changes in grid size will not affect the solution.

3.3 Solver Parameter and FSI Algorithm

The solver parameter for the current study is presented in Table 4. A co-simulation-based FSI coupling method was adopted in this study. The serial-based coupling method was adopted where RANS equation-based CFD solver[19] adapted for hydrodynamic parameters and will initiate the solution. FEM-based solver for hydro-structural analysis follows after reaching the rendezvous time, and data will be exchanged at this point. In step 1, the fluid solver initiates and solves for flow variables for a given time step, Δt and hydrodynamic forces are determined. In Step 2, these hydrodynamic forces are transferred from the fluid solver to the solid solver while the fluid solver waits. These forces are applied to the structural model, and the deformation and stresses are solved by the structural solver in Step 3. In Step 4, these deformations are transferred from the solid solver to the fluid solver. Steps 1 to 4 repeat to form an "FSI cycle, " constituting one coupling step. At the end of each coupling step, the solution quantities are up to date. The solution is marched till a steady state is reached. Figure 4 demonstrate the FSI cycle for Co-Simulation coupling. Further details about the coupling algorithm can be found in Kumar[6], *et al.*

Table 5. Solver parameter

Parameter	Settings
Solver	Three-dimensional, Unsteady and Segregated flow
Turbulence model	k-ω
Wall treatment	Two-layer wall Y+ treatment
Phase	Single phase
FSI	Co-Simulation
Others	Morphing, RBF, MRF

4. RESULTS AND DISCUSSION

The hydrodynamic performance parameters of the propeller geometry, such as thrust coefficient (K_T), torque coefficient (K_Q) at with wake and open water efficiency (η_o), were obtained for various advance coefficients (J) using CFD as a part of validation study numerical simulation. The study was carried out to predict the hydroelastic performance of a flexible marine propeller using co-simulation studies for a

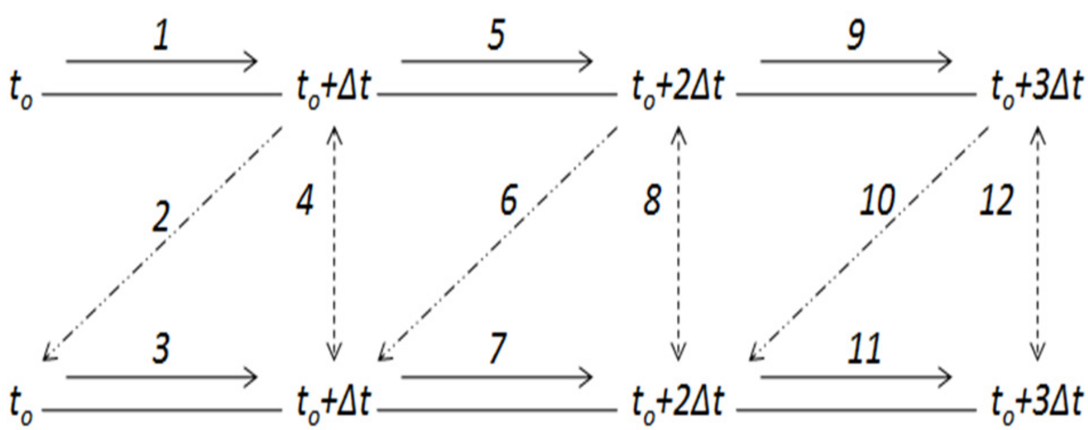

Figure 4. FSI cycle.

Potsdam Propeller Test Case (PPTC) P1790 propeller operating at open water conditions. Figure 4 illustrates the observation of displacement of PPTC propeller using current method and literature (experimental and numerical). It is very clearly identified that the data obtained using the current method very much accurate in both hydrodynamic and hydroelasticity aspect. Table 6 illustrates the results of hydrodynamic data at various advance ratio for validation of numerical study. The following equations explains the estimation of thrust, torque and open water coefficients.

$$K_T = \frac{T}{\rho n^2 d^4} \quad (1)$$

$$K_Q = \frac{Q}{\rho n^2 d^5} \quad (2)$$

$$\eta_0 = \frac{K_T J}{K_Q 2\pi} \quad (3)$$

where, T is the thrust, Q is torque, d is propeller diameter, n is revolution per second, ρ is the density of fluid, J is advance ratio.

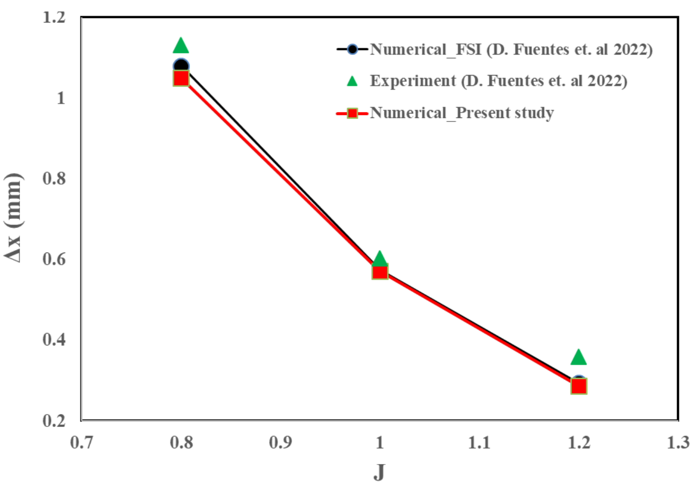

Figure 5. Hydrodynamic performance curves in open water conditions for homogeneous and composite propeller.

The numerical FSI analysis of metal and two FRP propellers was carried out. The wall Y+ value for the Aluminium propeller is shown in Fig. 5. The values are found to be well within the limits. The performance analysis of the propeller was computed in terms of hydrodynamic coefficients, i.e. thrust, torque and efficiency. The propeller was set to revolve in its design RPM, and thrust and torque were measured. The hydroelastic performance with two different stacking sequences and three different materials under the influence of wake is discussed below. Figure 5 illustrates the Wall Y+ values on propeller blades.

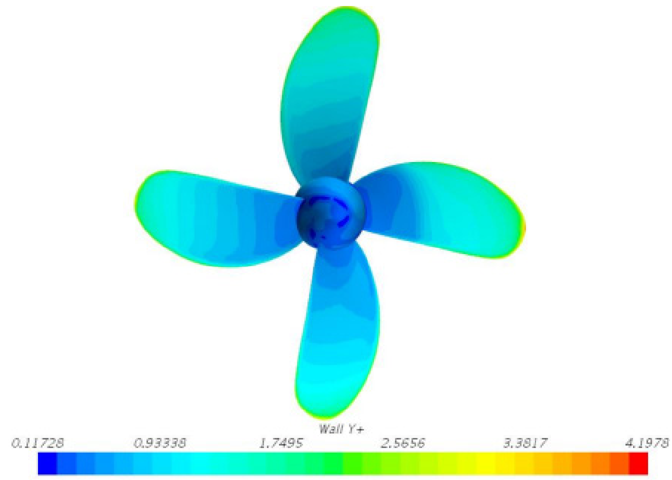

Figure 6. Wall Y+ Value.

Figure 6 illustrates the wake influenced tip hydroelastic tip displacement at the operating condition for Al propeller. Figure 7 and Fig. 8 depicts the displacement at the tip for stacking sequences A for CFRP and GFRP material respectively Figure 9 and Figure 10 depicts the displacement at the tip for stacking sequences B for CFRP and GFRP material respectively. The thrust and torque coefficients were measured at the design advance coefficient under the influence of the non-uniform wake created by the hull form. Table 7 illustrates the hydrodynamic and hydroelastic performance parameters for all the propeller material. The behind hull propeller efficiency was found to be maximum under the influence of wake with GFRP A sequence followed by GFRP B. However, FRP propeller found to have increased efficacy than Al propeller. The FRP has outperformed the Al propeller material under wake regime in hydrodynamic aspect with increased thrust and efficacy.

Table 6. Hydrodynamic parameter of the PPTC propeller at different advance ratios

Advance ratio (J)	0.8	1	1.2
Numerical_FSI (D. Fuentes, *et al.* 2022) (K_T)	0.55	0.4	0.28
Experiment (D.Fuentes, *et al.* 2022) (K_T)	0.53	0.38	0.27
Numerical_Present study (K_T)	***0.52***	***0.38***	***0.26***
Numerical_FSI (D.Fuentes, *et al.* 2022) ($10K_Q$)	1.31	1.03	0.79
Experiment (D. Fuentes, *et al.* 2022) ($10K_Q$)	1.3	1.05	0.81
Numerical_Present study ($10K_Q$)	***1.27***	***1.03***	***0.8***
Numerical_FSI (D.Fuentes, *et al.* 2022)_Deflection	1.08	0.58	0.29
Experiment (D.Fuentes, *et al.* 2022)_Deflection	1.13	0.6	0.36
Numerical_Present study_Deflection	***1.05***	***0.57***	***0.29***
Percentage error with experiment (Thrust)	-1.92	-0.16	-1.61
Percentage error with experiment (Torque)	-2.3	-1.63	-1.1

Table 7. FSI results with various staking sequence CFRP in wake

Material	AL	CFRP A	CFRP B	GFRP A	GFRP B
K_{TH}	0.19	0.205	0.211	0.221	0.210
$10K_{QH}$	0.628	0.60	0.550	0.52	0.520
η_H	0.245	0.274	0.300	0.324	0.322
Tip displacement [mm]	0.07599	0.027	0.010	0.095	0.220
Maximum stress [MPa]	8.77	6.236	6.400	7.674	7.747

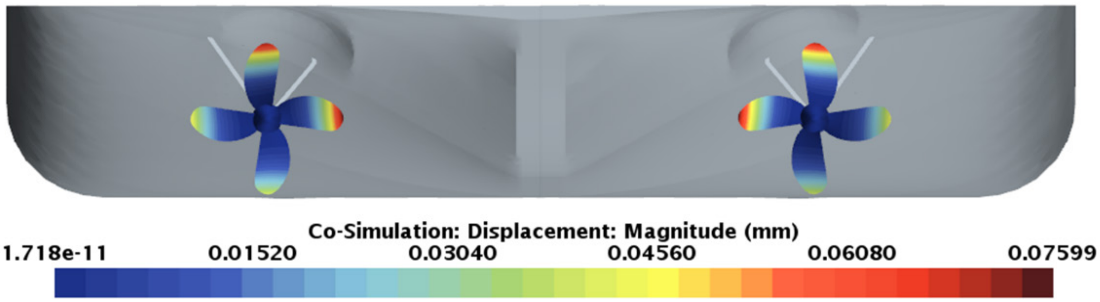

Figure 7. Tip displacement for Al.

Figure 8. CFRP displacement for sequence A.

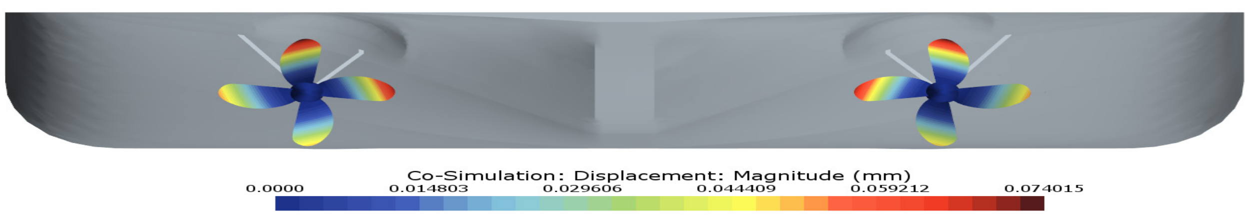

Figure 9. GFRP displacement for Sequence A.

Figure 10. CFRP displacement for Sequence B.

Figure 11. GFRP displacement for Sequence B.

Thus, it is well established that the deformation alters the blade profile and the efficacy. The von Mises stress was established for all the material as illustrated in Table 7 and found to be less than homogeneous metal. Also, it is very much evident that the unlike open water, influence of wake is highly heterogeneous and reflected in the blade profile deformation.

5. CONCLUSION

The numerical study was completed to understand the wake characteristics and their effect on the hydroelastic performance of a Wageningen B series propeller. Three different propeller materials with different stacking sequence were tested for FSI performances, and the following conclusion can be drawn from the study.

- Two composite propellers were tested for their FSI performance with identical geometry. The hydrodynamic performance was measured for all three propellers, and found that the GF propeller has a higher thrust coefficient
- The hydrodynamic thrust found to be slightly increased with GFRP A sequence compared to all the materials and Al as least
- The displacement of FRP and Al is heterogeneous
- The influence of stacking sequence was observed in the hydroelastic properties
- There have been marginal differences in the stress values for all the material due to minimal change in the geometry and blade profile.

Hence it can be concluded that the FRP propeller are very much efficient than the isotropic material under the influence of wake. Also further study has to be carried out to identify the influence of stacking sequencing in obtaining hydrodynamic efficiency at off design conditions.

REFERENCES

1. He, X.D.; Hong, Y. & Wang, R.G. Hydroelastic optimisation of a composite marine propeller in a non-uniform wake. *Ocean Engineering*, 2012, **39**, 14–23. doi: 10.1016/j.oceaneng.2011.10.007
2. Han, S.; Lee, H. & Min, Churl S. Investigation of hydro-elastic performance of marine propellers using fluid-structure interaction analysis. *In* Proceedings of the ASME 2015 International Mechanical Engineering Congress and Exposition. Vol. 7A*:* Fluids Engineering Systems and Technologies. Houston, Texas, USA. November 13–19, 2015. V07AT09A038. ASME, pp. 1–9. doi: 10.1115/IMECE2015-51089
3. Zondervan, Gert-Jan.; Grasso, N. & Lafeber, Wim. Hydrodynamic design and model testing techniques for composite ship propellers. *In:* Proceedings of the Fifth International Symposium on Marine Propulsors, 2017, pp. 1–9.
4. Grasso, N.; Hallmann, R. & Scholcz, T. Measurements of the hydro-elastic behaviour of flexible composite propellers in non-uniform flow at model and full scale. *In* Sixth International Symposium on Marine Propulsor*s*, 2019, Rome. Available at :www.refresco.org
5. Ashok, Kumar S.; Anantha, Subramanian V. & Vijayakumar, R. Numerical study on the performance analysis and vibration characteristics of flexible marine propeller. *In* Proceedings of the ASME 2020 39th International Conference on Ocean, Offshore and Arctic Engineering. *Ocean Engineering.,* 2020*,* 6A, pp. 3–7. doi: 10.1115/OMAE2020-18538
6. Kumar, Ashok.; Vijayakumar, R. & Subramanian, V. Numerical fluid-structure interaction analysis for a flexible marine propeller using co-simulation method. *Int. J. Maritime Engin.,* 2021, **163,** 83–92. doi: 10.5750/ijme.v163iA2.759
7. Ashok, Kumar S. & Vijayakumar, R. Numerical study on the performance of a composite marine propeller in self-propulsion condition using the FSI algorithm. *OCEANS,* 2022, 1-6. doi: 10.1109/OCEANSChennai45887.2022.9775126.
8. Liang, L.; Baoji, Z. & Hao, Z. Hydrodynamic performance optimisation of marine propellers based on fluid-structure coupling. *Brodogradnja,* 2023, **74**, 145–164. doi: 10.21278/brod74308
9. Majumder, P. & Maity, S. A critical review of different works on marine propellers over the last three decades. *Ships & Offshore Struct.,* 2023, **18**, 391–413. doi: 10.1080/17445302.2022.2058767
10. Lianzhou, Wang.; Tiecheng, Wu.; Jie, Gong. & Yiren, Yang. Numerical analysis of the wake dynamics of a propeller. *Physics of Fluids,* 2021, **33**(9), 095120. doi : 10.1063/5.0064100.
11. Felli, Mario.; Di, Felice Fabio. Guj, Giulio. & Camussi, Roberto, Analysis of the propeller wake evolution by pressure and velocity phase measurements. *Experimental Fluids,* 2006, **41**, 441–451. doi: 10.1007/s00348-006-0171-4
12. Nouri, N.M.; Mohammadi, S.; Neyestanaki, M.K. & Beygi, E. Hydroelastic effects of the camber ratio on a ducted marine propeller in a wake flow. *J. of Appl. Mechanic. Techical Physics,* 2018, **59**, 445–450. doi: 10.1134/S0021894418030070
13. An, Xiaoyi.; Song, Baowei.; Xia, Hui.; Ding, Yongle.; Jin, Zihui. & Lessard, Larry. Coupled numerical simulation and modal analysis of composite ducted propeller. *In* Sixth International Symposium on Marine Propulsors. Rome, 2019.
14. An, Xiaoyi.; Wang, Peng.; Song, Baowei. & Larry, Lesssard. Bi-directional fluid-structure interaction for prediction of tip clearance influence on a composite ducted propeller. *Ocean Engineering,* 2020, **208**, 107390. doi: 10.1016/j.oceaneng.2020.107390
15. Han, Shiyu.; Wang, Peng.; Jin, Zhihui.; An, Xiaoyi. & Hui, Xia. Structural design of the composite blades for a marine ducted propeller based on a two-way fluid-structure interaction method. *Ocean Engineering,* 2022, **259**, 111872. doi: 10.1016/j.oceaneng.2022.111872
16. Hussain, Mohamed.; Abdel-Nasser, Yehia.; Banawan, Adel. & Ahmed, M.Y. Failure analysis of tapered composite propeller blade. *Ocean Engineering* 2021, **236,** 109506.

doi: 10.1016/j.oceaneng.2021.109506

17. Fuentes, D.; Cura, Hochbaum A. & Schulze, R. Numerical and experimental fluid–structure interaction analysis of a flexible propeller. *Ship Technol. Res.*, 2022, 1–11. doi: 10.1080/09377255.2022.2115241
18. Roache, P.J. Perspective: A method for unform reporting of Grid refinement studies. *J. Fluid Engin.,* 1994, **116**, 405–413. doi: 10.1115/1.2910291
19. Siemens Digital Industries, Software. Simcenter STAR-CCM+User Guide, version 2021.1, (2021).
20. Oosterveld MWC, & van Oossanen P. Further computer-analyzed Dat of the Wageningen B-Screw Series. *Int. Shipbuilding Progress*, 1975, **22**, 251–262.

ACKNOWLEDGEMENTS

The authors would like to thank the Science and Engineering Research Board (SERB), Govt. of India, for supporting this work via the project 'FILE NO.CRG/2022/001718'. The authors would also like to thank the High-Performance Computation Environment (HPCE) of IIT Madras for its computational resources.

CONTRIBUTORS

Dr Ashok Kumar obtained his PhD degree in the field of Naval Architecture and Ocean Engineering at the Department of Ocean Engineering, IIT, Madras. His research interests include: Ship design, hydrodynamics, propellers, composite materials, motion analysis of floating structures etc.
In this paper, he has investigated the research topic, developed the methodology, performed formal analysis and visualisation, written the original draft, edited, and reviewed the manuscript.

Cdr (Dr) (Rted.) R. Vijayakumar (Indian Navy) obtained his PhD from IIT Delhi. He is presently working as a Professor at Dept. of Ocean Engineering at IIT, Madras. His areas of interest include: Warship design, ship hydrodynamics, Ship dynamics and Computational Fluid Dynamics (CFD). In the current study, he has guided the analysis and interpretation of the data and manuscript preparation.